Alveolar rhabdomyosarcomas in conditional *Pax3:Fkhr* mice: cooperativity of Ink4a/ARF and Trp53 loss of function

Charles Keller,[1] Benjamin R. Arenkiel,[2] Cheryl M. Coffin,[3] Nabeel El-Bardeesy,[5] Ronald A. DePinho,[5] and Mario R. Capecchi[4,6]

[1]Division of Pediatric Hematology-Oncology and Department of Pediatrics, [2]Department of Human Genetics, [3]Division of Pediatric Pathology and Department of Pathology, and [4]Howard Hughes Medical Institute and Department of Human Genetics, University of Utah, Salt Lake City, Utah 84112, USA; [5]Department of Medical Oncology, Dana-Farber Cancer Institute, Department of Medicine, and Department of Genetics, Harvard Medical School, Boston, Massachusetts 02115, USA

Alveolar rhabdomyosarcoma is an aggressive childhood muscle cancer for which outcomes are poor when the disease is advanced. Although well-developed mouse models exist for embryonal and pleomorphic rhabdomyosarcomas, neither a spontaneous nor a transgenic mouse model of alveolar rhabdomyosarcoma has yet been reported. We report the first mouse model of alveolar rhabdomyosarcoma using a conditional *Pax3:Fkhr* knock-in allele whose activation in late embryogenesis and postnatally is targeted to terminally differentiating *Myf6*-expressing skeletal muscle. In these mice, alveolar rhabdomyosarcomas occur but at low frequency, and *Fkhr* haploinsufficiency does not appear to accelerate tumorigenesis. However, *Pax3:Fkhr* homozygosity with accompanying Ink4a/ARF or Trp53 pathway disruption, by means of conditional *Trp53* or *Ink4a/ARF* loss of function, substantially increases the frequencies of tumor formation. These results of successful tumor generation postnatally from a target pool of differentiating myofibers are in sharp contrast to the birth defects and lack of tumors for mice with prenatal and postnatal satellite cell triggering of *Pax3:Fkhr*. Furthermore, these murine alveolar rhabdomyosarcomas have an immunohistochemical profile similar to human alveolar rhabdomyosarcoma, suggesting that this conditional mouse model will be relevant to study of the disease and will be useful for preclinical therapeutic testing.

[*Keywords*: Alveolar rhabdomyosarcoma; *Pax3:Fkhr*; *Pax3*; *Fkhr*; *FoxO1A*; chromosome translocation; satellite cell]

Supplemental material is available at http://www.genesdev.org.

Received July 26, 2004; revised version accepted September 3, 2004.

Rhabdomyosarcomas are a substantial problem in pediatric oncology. The most difficult patients to treat are those with unresectable local disease or metastases (Wexler and Helman 1997; Arndt and Crist 1999). Rhabdomyosarcomas are divided into two major histological subtypes, alveolar and embryonal (Arndt and Crist 1999). Alveolar histology is an independent predictor of worsened outcome, and children with metastatic alveolar rhabdomyosarcomas have a five-year survival rate <30% (Wexler and Helman 1997; Arndt and Crist 1999). The unique histological appearance and significantly worse prognosis for alveolar rhabdomyosarcomas compared with embryonal rhabdomyosarcoma suggest that alveolar rhabdomyosarcoma is biologically distinct from nonalveolar subtypes (e.g., embryonal). Furthermore, despite collaborative national trials of multimodal therapy and attempts at chemotherapy intensification, the outcome for patients with advanced stage alveolar rhabdomyosarcomas has not improved in more than two decades (Wexler and Helman 1997; Arndt and Crist 1999). This plateau in conventional treatments suggests that novel molecularly targeted therapy may be necessary to treat this tumor effectively.

The cell (or cells) of origin for alveolar rhabdomyosarcomas is unknown. The genes and proteins expressed by tumors are characteristic of both immature and well-differentiated embryonic and postembryonic muscle lin-

[6]Corresponding author.
E-MAIL mario.capecchi@genetics.utah.edu; FAX (801) 585-3425.
Article published online ahead of print. Article and publication date are at http://www.genesdev.org/cgi/doi/10.1101/gad.1244004.

eages (Tonin et al. 1991). Although congenital cases of alveolar rhabdomyosarcomas have been reported (Grundy et al. 2001), 84% of pediatric rhabdomyosarcomas arise after the first year of life (Gurney et al. 1999), suggesting either a long latency of an embryonically derived tumor precursor or, more likely, a postembryonic origin of the tumors. In the accompanying paper (Keller et al. 2004), we show that initiation of alveolar rhabdomyosarcoma from somite-derived myogenic precursors, the embryonic satellite cell pool, and the postnatal satellite cell pool does not occur in a mouse model. Therefore, our experimental design for this study was influenced strongly by the observation that the immunohistochemical profile of rhabdomyosarcomas is similar to differentiated, multinucleated skeletal muscle, and that the signature cell of rhabdomyosarcoma is the multinucleated rhabdomyoblast (Qualman et al. 1998).

Most alveolar rhabdomyosarcomas share a common genetic feature, the translocation-mediated fusion of a *Pax* gene to a *Fkhr* gene (Barr et al. 1993). The t(2;13)-mediated *Pax3:Fkhr* fusion gene is believed to play a key role in 55%–75% of alveolar rhabdomyosarcomas, whereas the t(1;13)-mediated *Pax7:Fkhr* fusion gene is believed to play a key role in 10%–22% of alveolar rhabdomyosarcomas (Sorensen et al. 2002). Both of these chimeric genes results in production of a novel transcription factor that has the DNA-binding domain from *Pax3* or *Pax7*, important regulators of muscle development, fused to the potent transactivation domain of the *Fkhr* tumor suppressor (Arndt and Crist 1999). These chimeric *Pax:Fkhr* genes are believed to result in a molecular gain of function that may in part lead to the initiation of an inappropriate muscle development program in the affected cells.

Our *Pax3:Fkhr* conditional knock-in allele builds on but is distinguished from previous informative germ-line *Pax3:Fkhr* models that do not generate tumors, because our model more carefully recapitulates the translocation-mediated genomic DNA rearrangement found in human tumors. Specifically, our model exchanges potentially important gene regulatory elements in the 3′ genomic region of *Pax3* for those from the 3′ genomic DNA of *Fkhr*. A Cre/LoxP-mediated translocation across heterologous chromosomes would represent the ideal method for modeling this cancer, and this approach has been successfully demonstrated for a leukemia model (Forster et al. 2003). However, because the *Pax3:Fkhr* fusion gene is not a robust oncogene in previous germ-line *Pax3:Fkhr* mice (Anderson et al. 2001; Lagutina et al. 2002; Relaix et al. 2003), other additional genetic events are likely required for alveolar rhabdomyosarcoma tumor progression. The much greater efficiency of the knock-in approach versus the chromosomal translocation approach (50% vs. 10^{-6}) permits generation of the fusion gene in a sufficient number of cells to allow for spontaneous occurrence of secondary genetic events at a reasonable frequency. Our model addresses these issues.

Conditional modeling of alveolar rhabdomyosarcoma in the mouse is especially attractive because of the strong association between *Pax3:Fkhr* and this somatic tumor. We have generated a Cre/LoxP-mediated conditional *Pax3:Fkhr* knock-in allele that can be triggered in distinct myogenic lineages by breeding to muscle-specific Cre drivers. In combination with a conditional *Fkhr* knockout allele generated for these studies, the Cre driver acts to recapitulate the t(2;13) human translocation by both activating *Pax3:Fkhr* and inactivating single normal alleles of *Pax3* and *Fkhr*. Other putative initiating events can also be triggered in a muscle-lineage-specific manner by breeding these alleles with mouse lines harboring conditional tumor suppressors or oncogenes.

Disruption of Ink4a/ARF and Trp53 pathways has been implicated as a cooperative effect for alveolar rhabdomyosarcomagenesis in humans (Felix et al. 1992; Takahashi et al. 2004) and for non-alveolar rhabdomyosarcomagenesis for humans with germ-line Trp53 mutations (Li-Fraumeni Syndrome) or sporadic tumors (Li and Fraumeni 1969) as well as for transgenic mouse models of embryonal and pleomorphic rhabdomyosarcoma (Jacks et al. 1994; Sharp et al. 2002; Fleischmann et al. 2003; Nanni et al. 2003). While Trp53 contributes to many cellular functions such as differentiation, angiogenesis, cellular senescence, and apoptosis (Kirkwood 2002), its overlapping role with the Ink4a/ARF locus controlling cell cycle withdrawal via the G1–S checkpoint is especially relevant when considering the potential cell of origin for rhabdomyosarcomas. Loss of replicative checkpoint would be advantageous not only to the expansion of a myogenic precursor transforming into rhabdomyosarcoma, but it would be especially critical to rhabdomyosarcomagenesis from terminally differentiating myofibers in quiescence.

In this study we report the first mouse model of alveolar rhabdomyosarcoma, which has been generated by conditional activation of *Pax3:Fkhr* and conditional inactivation of the Ink4a/Arf and Trp53 pathways in a target pool of terminally differentiating, *Myf6*-expressing skeletal muscle. These tumors closely recapitulate the histological features and immunohistochemical profile of human alveolar rhabdomyosarcomas. This report provides an important starting point for understanding the initiation and progression of this tumor and its potential cell(s) of origin.

Results

Design and generation of targeted mouse lines

The conditional *Pax3:Fkhr* (P3Fm) knock-in allele was designed to allow normal *Pax3* expression of that allele until Cre is present (Fig. 1A). With expression of Cre, this normally functioning *Pax3* allele is converted to a *Pax3:Fkhr* (P3Fa) allele, fusing exons 1–7 of *Pax3* to a 9.3-kb 3′ genomic region of the *Fkhr* locus containing *Fkhr* exon 2, exon 3, and 6.5 kb of the untranslated region and genomic DNA. Simultaneously, the *eYfp* fluorescent marker gene is activated as a second cistron downstream from an encephalomyocarditis virus-derived internal ribosome entry site (IRES). This design mimics the disease-associated translocation with respect

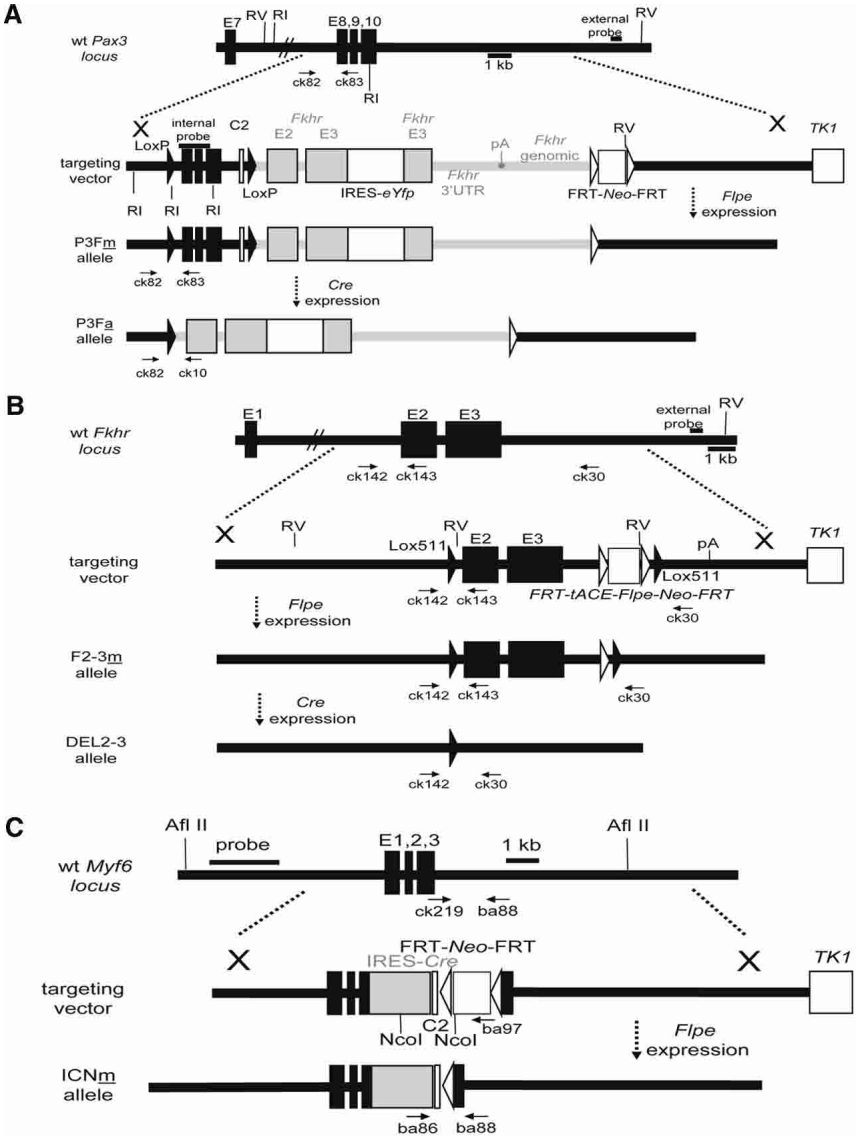

Figure 1. Structure of targeted alleles. (*A*) For the *Pax3:Fkhr*-targeted knock-in allele, a targeting vector was designed for the insertion of a complex cassette into the 3′-region of the *Pax3* gene, thereby modifying the last three of 10 exons. FRT sites flank the *neomycin resistance* gene (*Neo*) and allow excision of this gene upon breeding to an *Flp-e* mouse (Rodriguez et al. 2000). The P3Fp allele indicates the presence of the *neomycin resistance* gene (*Neo*$^+$), whereas the P3Fm allele indicated the absence of the *neomycin resistance* gene (*Neo*$^-$). LoxP sites flank exons 8–10 of *Pax3* as well as an inserted polyadenylation/stop signal from the *Complement2* (*C2*) gene. Prior to activation, the P3Fm allele will transcribe a full-length *Pax3* transcript. Upon activation by CRE, exons 8–10 and the stop signal are removed and exon 7 of *Pax3* is juxtaposed to exons 2 and 3 of *Fkhr*, thereby creating an activated *Pax3:Fkhr* fusion allele (*P3Fa*). An internal ribosomal entry site (IRES) downstream from *Fkhr* exon 3 allows for bicistronic expression of *eYFP*. The positions of PCR genotyping primers ck82, ck83, and ck10 are shown. (TK1) Thymidine kinase; (FRT) Flp-e recombinase recognition sequence; (RI) EcoRI restriction site; (RV) EcoRV restriction site; (UTR) untranslated region. (*B*) For the *Fkhr* conditional mouse line, a targeting vector was designed for which exons 2 and 3 were flanked by Lox511 sites. The F2-3p allele indicates the presence of the *neomycin resistance* gene (*Neo*$^+$), whereas the F2-3m allele indicates the absence of the *neomycin resistance* gene (*Neo*$^-$). In the presence of CRE, the inactivated DEL2-3 allele is generated. The positions of PCR genotyping primers ck142, ck143, and ck30 are shown. (*C*) For the *Myf6–Cre* allele, a targeting vector was designed for the insertion of a complex cassette into the 3′-region of the *Myf6* gene. At an engineered XhoI site in the 3′-UTR, an IRES–*Cre* was inserted to allow bicistronic expression of *Myf6* and *Cre*. An FRT–*Neo*–FRT cassette was inserted 3′ to IRES–*Cre*. The ICNp allele indicates the presence of the *neomycin resistance* gene (*Neo*$^+$), whereas the ICNm allele indicates its absence. The positions of PCR genotyping primers ck219, ba88, and ba86 are shown.

to *Pax3:Fkhr* expression being directed by the *Pax3* promoter, and being potentially influenced by 3′ *Fkhr cis*-regulatory elements knocked into the *Pax3* locus. Germline mice were established carrying the conditional *Neo*-containing *Pax3:Fkhr* allele (*Pax3*$^{P3Fp/wt}$) (data not shown). After removing the positive selection cassette by Flpe-mediated recombination, *Neo*-excised *Pax3*$^{P3Fm/wt}$ and *Pax3*$^{P3Fm/P3Fm}$ mice prove to be viable and fertile, breeding normally. Whereas mice and humans heterozygous for *Pax3* loss-of-function mutations are readily discernable because of their deficiencies of melanocyte production (Goulding et al. 1993; Tassabehji et al. 1993), *Pax3*$^{P3Fm/wt}$ mice without Cre resemble wild-type mice and have normal coat color pigmentation. It therefore appears that, in the absence of Cre, the targeted modifications introduced into the *Pax3* locus do not affect normal Pax3 function.

The *Fkhr* conditional knockout allele was designed to allow normal expression of that allele until Cre is present (Fig. 1B). Upon Cre expression, this functionally normal *Fkhr* allele is inactivated by excision of exons 2 and 3 removing the DNA-binding domain and the full transactivation domain of the *Fkhr* gene. Germ-line mice were established and confirmed by Southern analysis to carry the conditional *Neo*-containing allele (*Fkhr*$^{F2\text{-}3p/WT}$) (data not shown). The *Neo*-excised *Fkhr*$^{F2\text{-}3m/WT}$ and *Fkhr*$^{F2\text{-}3m/F2\text{-}3m}$ mice are viable and fertile, breeding normally. Homozygous *Fkhr*$^{DEL2\text{-}3/DEL2\text{-}3}$ mice with germ-line absence of both *Fkhr* alleles die by embryonic day 10 (E10) (data not shown), consistent with previous

reports for nonconditional *Fkhr* alleles (Hosaka et al. 2004).

To allow *Cre* expression in a target pool of differentiating skeletal muscle following the endogenous expression pattern of *Myf6* (Fig. 1C), we designed an Myf6–Cre allele. This allele expresses *Cre* as a second cistron from an IRES downstream from the *Myf6* gene. Germ-line mice carrying this allele were established (data not shown). Unlike previously reported mice with 3′ *Myf6* modifications that alter the normal expression of *Myf6* and/or adjacent *Myf5* gene (Olson et al. 1996), our $Myf6^{ICNm/WT}$ and $Myf6^{ICNm/ICNm}$ mice are viable and fertile as both heterozygotes and homozygotes, breeding normally. By small animal computed tomography, these animals also lacked the rib abnormalities (data not shown) previously seen in Myf6/Myf5 loss-of-function alleles (Braun and Arnold 1995).

To test the muscle-specific pattern of expression of our *Myf6–Cre* alleles, we crossed mice carrying the *Myf6–Cre* allele to mice carrying the Rosa26 LacZ reporter (Sorriano 1999). In the latter mouse, production of LacZ mRNA is blocked by a strong polyadenylation signal flanked by LoxP sites. In the presence of Cre, the blocking cassette is excised and LacZ mRNA and β-galactosidase protein are synthesized. Shown in Figure 2A is whole-mount β-galactosidase staining of an E15.5 embryo heterozygous for both alleles ($Myf6^{ICNm/WT}$ $Gtrosa26^{tm1Sor/WT}$). Embryos of this genotype exhibit a skeletal-muscle-specific pattern of Cre expression. To confirm that the *Myf6–Cre* allele was expressed in the target pool of terminally differentiating myofibers, and not in satellite cells, we looked for coexpression of nuclear proteins Cre and Pax7 in $Myf6^{ICNm/WT}$ mice by immunohistochemistry in cross-section of skeletal muscle of 3-week-old mice. Non-overlap of these markers in Figure 2B demonstrates that Cre is not present in Pax7-expressing satellite cells; however, immunohistochemistry for Cre and myogenic transcription factor MyoD in Figure 2C demonstrates coexpression of these markers in the same nuclei as has been previously shown for postnatal terminally differentiating myofibers (Cornelison and Wold 1997).

Conditional production of the Pax3:Fkhr fusion protein in skeletal muscle

To generate the Pax3:Fkhr protein in skeletal muscle, we crossed mice carrying the *Pax3:Fkhr* knock-in allele to mice carrying the *Myf6–Cre* allele. $Pax3^{P3Fa/WT}$ $Myf6^{ICNm/WT}$ offspring were viable, fertile, and present in Mendelian ratios. To visualize the extent of Cre-induced formation of the *Pax3:Fkhr* fusion gene in skeletal muscle, we harvested the vastus lateralis muscle from these mice as well as from control mice and examined the expression of the *Pax3:Fkhr* reporter, eYFP. Epifluorescence microscopy of these muscles in cross-section showed eYFP expression in ~50% of the cells, suggesting that the Cre-mediated rearrangement of the *Pax3:Fkhr* locus was incomplete among mature muscle fibers (Fig. 2D), which is advantageous for demonstrating that tumors arise from *Pax3:Fkhr*-expressing cells.

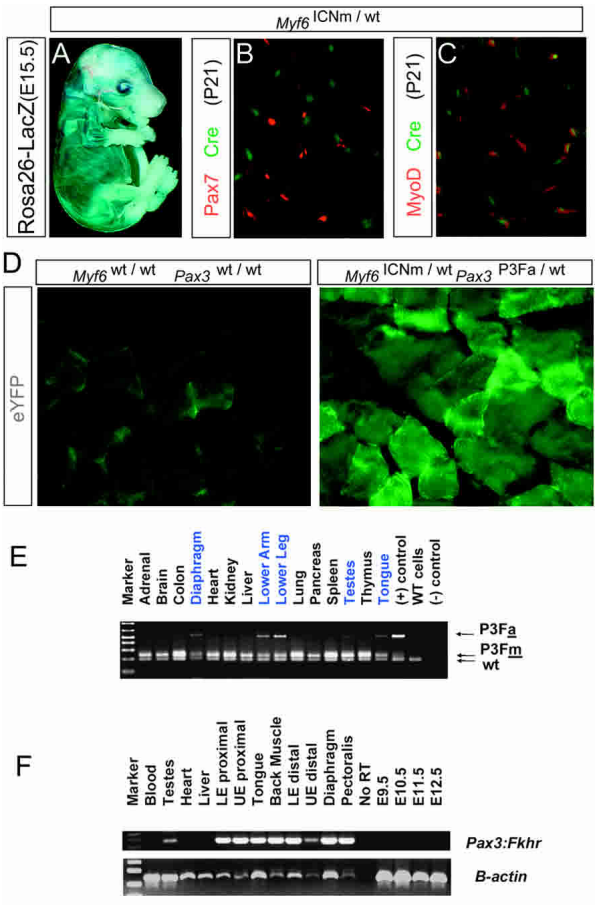

Figure 2. Characterization of the Pax3:Fkhr, Myf6–Cre experimental system. (*A*) The *Myf6–Cre* allele demonstrates a skeletal-muscle-specific pattern of expression in an E15.5 fetus carrying the ROSA26 *Cre*-activatable *LacZ* marker. (*B*) Nuclear-localized Cre (green) and the nuclear satellite cell marker Pax7 (red) are not coexpressed in cross-sectioned skeletal muscle of *Myf6–Cre* mice. (*C*) Cre and the post-satellite cell myogenic transcription factor MyoD are coexpressed in skeletal muscle of *Myf6–Cre* mice. (*D*) When crossed to the *Pax3:Fkhr* conditional knock-in allele, the *Myf6–Cre* allele causes heterogeneous expression of the *eYfp* marker of *Pax3:Fkhr* activation in cross-sectioned skeletal muscle of a 6-week-old mouse (*right*), with little autofluorescence in tissue of a control mouse (*left*). (*E*) Genomic DNA PCR of the *Pax3:Fkhr* locus from a 6-week-old mouse carrying the *Myf6–Cre* allele confirms heterogeneous activation of *Pax3:Fkhr* within each skeletal muscle sample from varying epaxial and hypaxial sites. Activation of *Pax3:Fkhr* in testes is noted. (*F*) RT–PCR of skeletal muscle tissue from a 6-week-old mouse carrying both the *Pax3:Fkhr* knock-in allele and the *Myf6–Cre* allele demonstrates *Pax3:Fkhr* transcript expression for the tissues shown to undergo genomic rearrangement of the *Pax3:Fkhr* knock-in allele.

To verify that the *Pax3:Fkhr* knock-in allele was being partially rearranged by the *Myf6–Cre* driver at the genomic level in a skeletal-muscle-specific manner, we performed PCR of genomic DNA from a variety of tissues from $Pax3^{P3Fa/WT}$ $Myf6^{ICNm/WT}$ animals. *Pax3:Fkhr*

rearrangements (Fig. 2E) were present not only in hypaxial skeletal muscle (lower leg, lower arm) but also in epaxial skeletal muscle (diaphragm, tongue). The *Pax3:Fkhr* allele was not rearranged in cardiac muscle, but a trace rearrangement was present in testes. However, the band for the unrearranged *Pax3:Fkhr* knock-in allele was still present in each skeletal muscle tissue tested, suggesting, as shown by *eYfp* microscopy of skeletal muscle, that the action of Cre occurred in ~50% of the differentiating skeletal muscle myofibers.

To confirm the presence of the *Pax3:Fkhr* transcript in skeletal muscle tissues of 6-week-old $Pax3^{P3Fa/WT}$ $Myf6^{ICNm/WT}$ mice, we performed nested RT–PCR using 5′ *Pax3* exon 6 and 3′ *Fkhr* exon 2 primers (Fig. 2F). Analysis revealed the expected pattern of hypaxial (upper and lower limb) and epaxial (tongue, back, diaphragm, and pectoralis) skeletal-muscle-specific *Pax3:Fkhr* expression, as well as trace expression in the testes. Nonspecific expression in cardiac muscle or liver was absent.

Mice expressing Pax3:Fkhr *develop alveolar rhabdomyosarcoma*

Mice carrying the *Pax3:Fkhr* knock-in allele and a *Myf6*-specific Cre driver were followed for up to 29 mo (Table 1). A tumor occurred in one of 228 animals at 12 mo of age. This tumor is shown in Figure 3A. Microscopic computed tomography (microCT) of the animal revealed the presence of a pedunculating tumor arising from the pectoralis major muscle, with stellate internal calcification suggestive of necrosis (Fig. 3B). On necropsy the tumor was highly vascular (Fig. 3C). Histology of the tumor at low magnification revealed the attachment of normal skeletal muscle at the tumor base (Fig. 3D). Higher power magnification revealed densely packed, small, round, blue cells with scant cytoplasm and corrugating vessels consistent with the solid variant of alveolar rhabdomyosarcoma (Fig. 3E). An example of the solid variant of alveolar rhabdomyosarcoma from human is shown in Figure 3F for comparison. The diagnosis was confirmed by positive immunohistochemistry for myogenin (Fig. 3G). Immunohistochemistry for smooth muscle actin and muscle-specific actin was also positive (data not shown). To provide supportive evidence that this tumor was nonsporadic, we genotyped two areas of the tumor, demonstrating that the conditional P3Fm allele had been clonally converted to the activated P3Fa allele (Fig. 3H), rather than exhibiting a nonactivated conditional allele or heterogeneity of nonactivated and activated alleles. Therefore, the tumor was derived from a Myf6–Cre-expressing cell.

Haploinsufficiency of Fkhr *does not significantly accelerate tumorigenesis*

The reciprocal chromosome 2 and 13 translocations observed in human alveolar rhabdomyosarcomas result in four genetic consequences: formation of the *Pax3:Fkhr* fusion gene, formation of the reciprocal *Fkhr:Pax3* fusion gene, loss of a single *Pax3* allele, and perhaps most significantly, the loss of a single *Fkhr* allele. To test the possibility that Fkhr loss contributes to the pathogenesis of alveolar rhabdomyosarcoma, we generated a conditional allele of *Fkhr* and introduced it into $Pax3^{P3Fa/WT}$ $Myf6^{ICNm/WT}$ mice. We followed 96 $Pax3^{P3Fa/WT}$ $Fkhr^{F2\text{-}3m/WT}$ $Myf6^{ICNm/WT}$ animals for up to 25 mo without the development of a

Table 1. *Mice generated for this study*

Genotype				(*n*)	Age (days) median, range	Tumor incidence	Onset (days)
Pax3:Fkhr heterozygote lines							
$Myf6^{ICNm/any}$	$Pax3^{P3Fa/WT}$	—	—	228	348, 35–889	1	383
$Myf6^{ICNm/any}$	$Pax3^{P3Fa/WT}$	$Fkhr^{F2\text{-}3m/WT}$	—	96	332, 49–739	0	NA
$Myf6^{ICNm/any}$	$Pax3^{P3Fa/WT}$	$Fkhr^{F2\text{-}3m/WT}$	$Trp53^{F2\text{-}10/WT}$	57	282, 76–406	0	NA
$Myf6^{ICNm/any}$	$Pax3^{P3Fa/WT}$	—	$Trp53^{F2\text{-}10/WT}$	16	235, 89–406	0	NA
$Myf6^{ICNm/any}$	$Pax3^{P3Fa/WT}$	—	$Trp53^{F2\text{-}10/F2\text{-}10}$	12	75, 65–295	0	NA
$Myf6^{ICNm/any}$	$Pax3^{P3Fa/WT}$	—	$Ink4a/ARF^{F2\text{-}3/WT}$	68	235, 16–393	0	NA
$Myf6^{ICNm/any}$	$Pax3^{P3Fa/WT}$	—	$Ink4a/ARF^{F2\text{-}3/F2\text{-}3}$	31	72, 47–295	0	NA
Control lines							
$Myf6^{ICNm/any}$	—	—	$Trp53^{F2\text{-}10/WT}$	50	262, 41–399	0	NA
$Myf6^{ICNm/any}$	—	—	$Trp53^{F2\text{-}10/F2\text{-}10}$	5	72, 57–303	0	NA
$Myf6^{ICNm/any}$	—	—	$Ink4a/ARF^{F2\text{-}3/WT}$	57	269, 41–388	0	NA
$Myf6^{ICNm/any}$	—	—	$Ink4a/ARF^{F2\text{-}3/F2\text{-}3}$	18	62, 41–295	0	NA
Pax3:Fkhr homozygote lines							
$Myf6^{ICNm/any}$	$Pax3^{P3Fa/P3Fa}$	—	—	36	219, 44–542	0	NA
$Myf6^{ICNm/any}$	$Pax3^{P3Fa/P3Fa}$	—	$Trp53^{F2\text{-}10/WT}$	12	216, 78–406	1	202
$Myf6^{ICNm/any}$	$Pax3^{P3Fa/P3Fa}$	—	$Trp53^{F2\text{-}10/F2\text{-}10}$	5	89, 72–295	2	75–91
$Myf6^{ICNm/any}$	$Pax3^{P3Fa/P3Fa}$	—	$Ink4a/ARF^{F2\text{-}3/WT}$	13	195, 66–295	0	NA
$Myf6^{ICNm/any}$	$Pax3^{P3Fa/P3Fa}$	—	$Ink4a/ARF^{F2\text{-}3/F2\text{-}3}$	14	72, 47–108	4	56–89

NA = not applicable.
any = *ICNm* or *WT* allele.

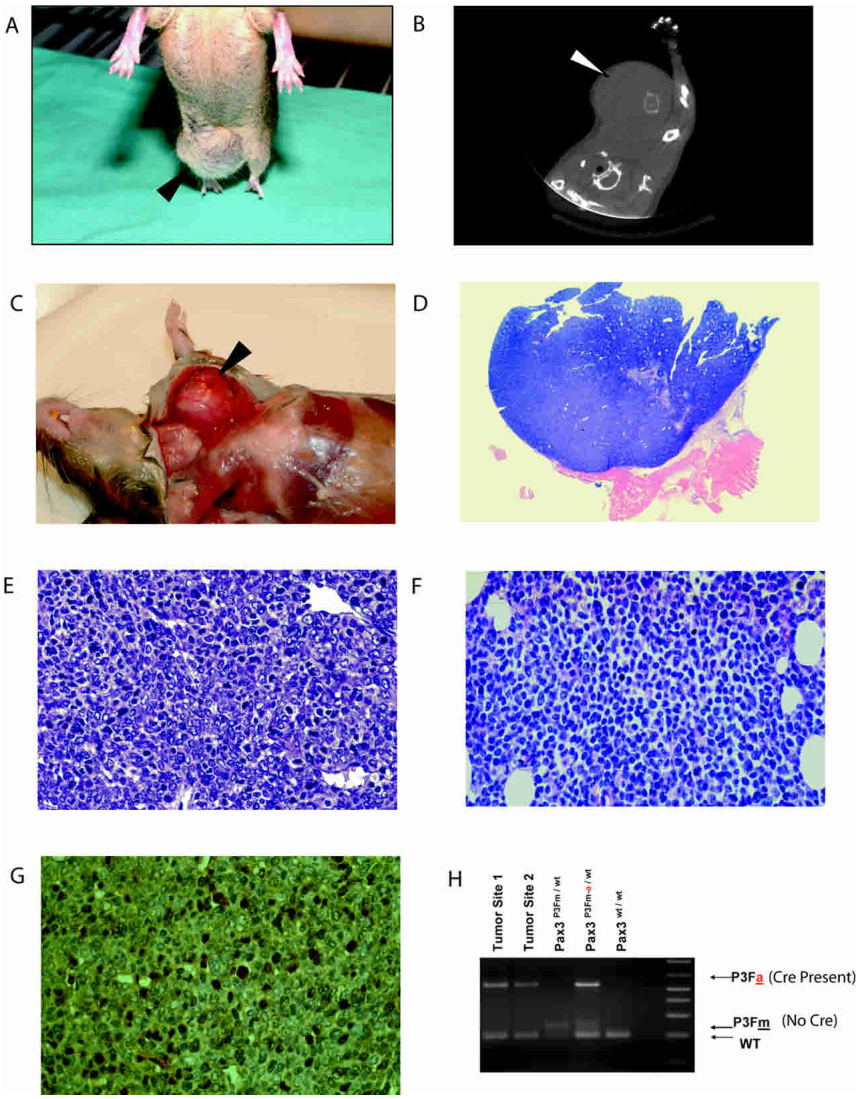

Figure 3. Alveolar rhabdomyosarcoma in Pax3:Fkhr Myf6–Cre mice. (*A*) A 12-month-old female *Pax3*$^{P3Fa/WT}$ *Myf6*$^{ICNm/WT}$ mouse was found to have a large mass (black arrowhead) arising from the left chest wall near the axilla. (*B*) Computed tomography scan revealed a well-circumscribed 13.8 × 6.4 × 9-mm mass (white arrowhead) arising from a more infiltrative base. A stellate area of calcification was indicative of central necrosis within the tumor. (*C*) Gross dissection revealed a highly vascular, rubbery tumor. (*D*) Low-power magnification of the hematoxylin- and eosin-stained tumor (blue) demonstrates adherent skeletal muscle (pink). (*E*) Higher-power magnification of the hematoxylin- and eosin-stained tumor shows densely packed cells with scant cytoplasm, consistent with the solid variant of alveolar rhabdomyosarcoma. (*F*) A human solid variant of alveolar rhabdomyosarcoma is shown for comparison. (*G*) Immunohistochemistry for myogenin is positive. (*H*) Genotyping of two areas of the tumor reveals clonal conversion of the conditional P3Fm allele to an activated P3Fa allele.

tumor (Table 1). We therefore concluded that haploinsufficiency of *Fkhr* does not significantly accelerate tumorigenesis when Pax3:Fkhr is expressed in the Myf6 domain for terminally differentiating skeletal muscle.

Ink4a/ARF and Trp53 mutations accelerate tumorigenesis

Because human alveolar rhabdomyosarcomas frequently carry mutations in the Ink4a/ARF and Trp53 pathways, we wished to test whether mutations that prominently affect G1–S cell cycle re-entry could accelerate the formation of alveolar rhabdomyosarcomas from a target pool of quiescent, terminally differentiating *Myf6*-expressing skeletal muscle. For this goal, we introduced conditional knockout alleles for *INK4a/ARF* (Aguirre et al. 2003) or *Trp53* (Jonkers et al. 2001) into our *Pax3:Fkhr* model. A total of 57 control mice with the genotype *Ink4a/ARF*$^{F2\text{-}3/WT}$ *Myf6*$^{ICNm/WT}$ and 50 mice with the genotype *Trp53*$^{F2\text{-}10/WT}$ *Myf6*$^{ICNm/WT}$ were followed for up to 13 mo without the development of alveolar rhabdomyosarcomas. We also followed 68 triple heterozygous *Pax3*$^{P3Fa/wt}$ *Ink4a/ARF*$^{F2\text{-}3/WT}$ *Myf6*$^{ICNm/WT}$ mice and 16 triple heterozygous *Pax3*$^{P3Fa/wt}$ *Trp53*$^{F2\text{-}10/WT}$ *Myf6*$^{ICNm/WT}$ animals for up to 13.5 mo without the development of a tumor (Table 1).

To increase the frequency of tumors, we began breeding for compound homozygotes. A total of 18 *Ink4a/ARF*$^{F2\text{-}3/F2\text{-}3}$ *Myf6*$^{ICNm/WT}$ control mice and five *Trp53*$^{F2\text{-}10/F2\text{-}10}$ *Myf6*$^{ICNm/WT}$ control mice remain cancer-free for 10 mo. However, in our first animal homozygous for the *Pax3:Fkhr* knock-in allele and homozygous for the *INK4a/ARF* knockout allele, we observed a soft tissue mass arising from the tongue base (Fig. 4A) at age 3 mo. MicroCT revealed a large neck mass encasing the trachea (Fig. 4B), which was also evident on necropsy (Fig. 4C). Histology of this tumor revealed classic alveolar rhabdomyosarcoma with entrapped normal skeletal muscle (Fig. 4D). Immunohistochemistry revealed the

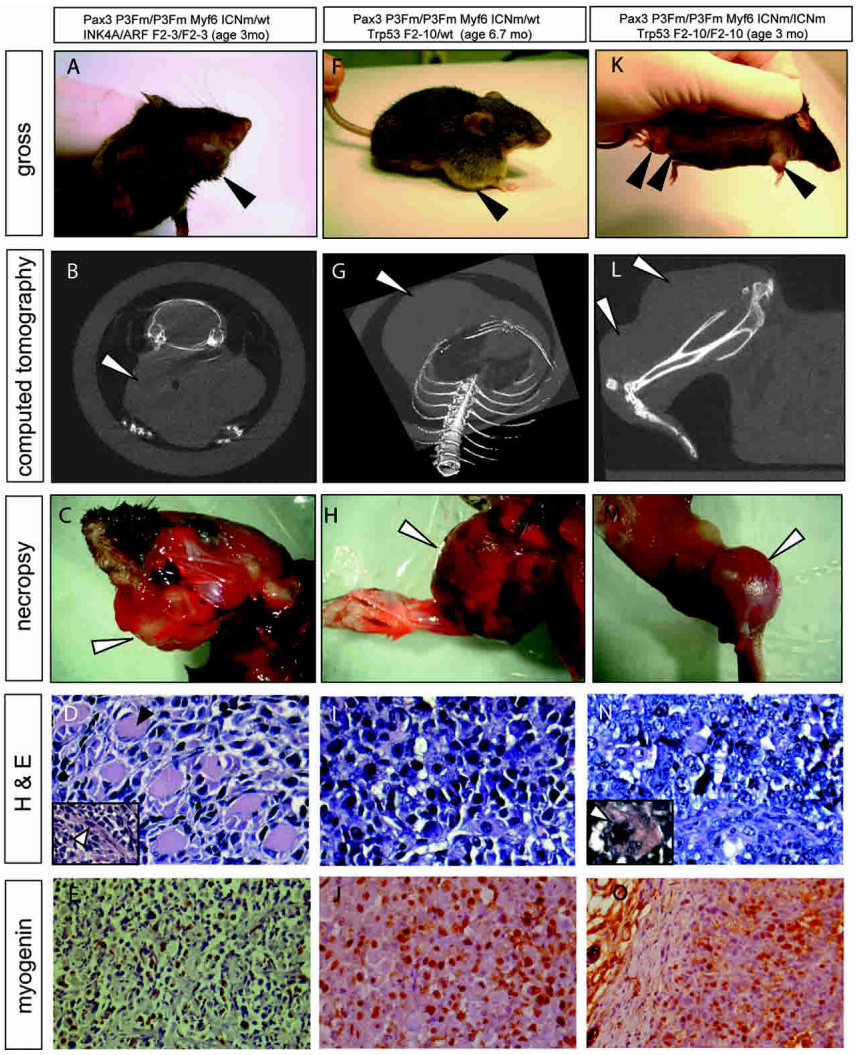

Figure 4. Alveolar rhabdomyosarcoma in Pax3:Fkhr Myf6–Cre mice with cell cycle control mutations. Three animals with Trp53 or Ink4a/ARF mutations that have developed classical alveolar rhabdomyosarcomas. (*A*,*F*,*K*) Gross appearance of the tumors of the tongue/jaw, chest/arm, and upper and lower extremities, respectively, marked with black arrowheads. (*B*,*G*,*L*) MicroCT of the tumor(s) for each animal demarcated by white arrows. (*C*,*H*,*M*) Appearance of the tumors (white arrowheads) at necropsy. (*D*,*I*,*N*) Hematoxylin and eosin staining of the tumors demonstrating classical alveolar histology and entrapped skeletal muscle (*D*, black arrowhead), strap cell (*D*, *inset*), and multinucleated rhabdomyoblasts (*N*, *inset*). (*E*,*J*,*O*) Immunohistochemistry for myogenin was positive for each tumor.

tumor to be myogenin positive, confirming the histological diagnosis. Three more mice with the identical genotype have also developed unifocal alveolar rhabdomyosarcomas of the masseter, neck, or anterior chest wall at age 2 mo (data not shown).

Because the *INK4a/ARF* gene products influence both Trp53 and pRb pathways, we sought to determine which pathway was primarily responsible for rhabdomyosarcomagenesis. We began breeding for mice with compound conditional *Pax3:Fkhr* homozygous alleles and conditional *Trp53* alleles. In these mice, we observed a soft tissue tumor arising from the right pectoralis major muscle of a 6.7-month-old $Pax3^{P3Fa/P3Fa}$ $Trp53^{F2\text{-}10/wt}$ $Myf6^{ICNm/WT}$ animal (Fig. 4F–H). Histology of this tumor revealed classic alveolar rhabdomyosarcoma (Fig. 4I). As was the case for the prior tumor, numerous multinucleated rhabdomyoblasts were present. Immunohistochemistry revealed the tumor to be myogenin positive, confirming the histological diagnosis. In a second mouse that was homozygous instead of heterozygous for the conditional *Trp53* allele, we observed earlier onset (age 3 mo) for four multifocal tumors arising from three extremities (Fig. 4K–M). These tumors also exhibited classic alveolar rhabdomyosarcoma histology and myogenin immunopositivity (Fig. 4N,O). An identical pattern of multifocal limb tumors was observed in a 2.5-month-old animal of the same genotype. By immunohistochemistry, Trp53 was absent from each of these alveolar rhabdomyosarcomas from Ink4a/ARF or Trp53 animals. We therefore suggest that Trp53 pathway disruption, either for its cell cycle control role or other roles, contributes to alveolar rhabdomyosarcoma formation in *Pax3:Fkhr* mice.

To answer the underlying question whether homozygosity for *Pax3:Fkhr* was a necessary and sufficient event for tumor formation in this model, irrespective of Trp53 or Ink4a/ARF mutations, we observed 36 double homozygote $Pax3^{P3Fa/P3Fa}$ $Myf6^{ICNm/ICNm}$ mice for up to 18 mo without the formation of tumors; however, a small number of mice with homozygous deletion of *Ink4a/ARF* or *Trp53* and only a heterozygous *Pax3:Fkhr* allele have not developed tumors within the same period of time as animals with homozygous deletion of *Ink4a/ARF* or *Trp53* and homozygous *Pax3:Fkhr* alleles, sug-

gesting for this mouse model that two *Pax3:Fkhr* alleles may be required for tumorigenesis.

Murine alveolar rhabdomyosarcomas have an immunohistochemical profile similar to human alveolar rhabdomyosarcomas

To assess the similarity of this preclinical model of alveolar rhabdomyosarcoma to the human disease, we examined the immunohistochemical profile of the murine tumors. A summary is presented in Table 2, and representative staining for $Pax3^{P3Fa/wt}$ $Ink4a/ARF^{F2\text{-}3/WT}$ $Myf6^{ICNm/WT}$ tumors is shown in Figure 5. The hepatocyte growth factor receptor, c-Met, is a known downstream target of Pax3:Fkhr expressed by alveolar rhabdomyosarcomas (Ginsberg et al. 1998) and was focally present in all murine alveolar rhabdomyosarcomas (Table 2; Fig. 5A). Pax7 expression was also present in murine alveolar rhabdomyosarcomas (Fig. 5B), as has been reported for many human alveolar rhabdomyosarcomas, albeit at low levels (Tiffin et al. 2003; Tomescu et al. 2004). In human alveolar rhabdomyosarcoma samples we tested, Pax7 expression comparable or greater than our murine tumors was seen in 6 of 32 cases (see Supplementary Fig. S1A). Similarly, the human rhabdomyosarcoma marker MyoD (Tonin et al. 1991) was uniformly expressed in the murine tumors (Fig. 5C). Trp53 was expressed in the tumor without *Trp53* or *Ink4a/ARF* conditional deletion, but a distinction could not be made between wild-type and mutated Trp53 (Table 2). In this tumor, murine p19ARF was not expressed (data not shown), suggesting that Trp53 function was intact. Nevertheless, the downstream effector of G1–S cell cycle reentry, Cyclin D1 (Cavenee 2002), was strongly expressed in all murine alveolar rhabdomyosarcomas (Fig. 5D). C-MYC, a proliferative factor expressed in some human alveolar rhabdomyosarcomas (Kouraklis et al. 1999) that often accompanies an apoptotic defect (Nilsson and Cleveland 2003), was strongly expressed in murine alveolar rhabdomyosarcomas for all genotypes (Fig. 5E) at comparable levels to the human rhabdomyosarcomas we tested (see Supplementary Fig. S1B); furthermore, the *Pax3:Fkhr* target gene and antiapoptotic factor Bcl-XL (Margue et al. 2000) was uniformly expressed across all murine rhabdomyosarcomas (Fig. 5F). A less common marker of human alveolar rhabdomyosarcomas, Neu (Mark et al. 1998), was absent from all murine *Pax3:Fkhr*-expressing tumors. CD44, a favorable prognostic marker of human rhabdomyosarcomas that is typically absent from alveolar rhabdomyosarcomas (Humphrey et al. 1999), was also absent in the murine alveolar rhabdomyosarcomas.

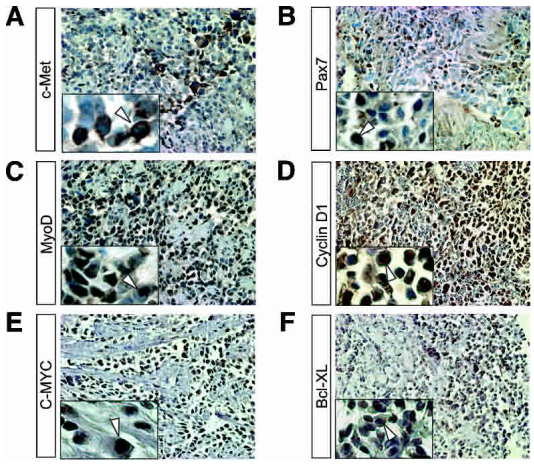

Figure 5. Representative immunohistochemical profile of alveolar rhabdomyosarcomas from $Pax3^{P3Fa/wt}$ $Ink4a/ARF^{F2\text{-}3/WT}$ $Myf6^{ICNm/WT}$ mice. Tumors expressed myogenic markers common to human alveolar rhabdomyosarcomas, including c-Met (*A*), Pax7 (*B*), and MyoD (*C*). (*D*) The cell cycle re-entry marker, Cyclin D1, was strongly expressed. (*E*) Other markers common to human and mouse alveolar rhabdomyosarcomas included C-MYC. (*F*) The anti-apoptotic protein, Bcl-XL, was strongly expressed and appeared to localize to the nuclear membrane as has been previously reported (Hsu et al. 1997). (*Insets*) Higher magnification of positively staining cells (white arrowhead).

Discussion

The alveolar subtype of rhabdomyosarcoma portends a poor prognosis when the disease is advanced (Wexler and Helman 1997). Although well-characterized embryonal and pleomorphic rhabdomyosarcomas mouse models exist, neither a spontaneous nor a transgenic mouse model of alveolar rhabdomyosarcoma has yet been reported. In this manuscript we report a faithful model of alveolar rhabdomyosarcoma built on the signature genetic change of this tumor. Using conditional mutagenesis to simulate events that occur as a result of a t(2;13) translocation associated with human alveolar rhabdomyosarcomas, we have been able to convert a functionally nor-

Table 2. *Immunohistochemical profile of murine alveolar rhabdomyosarcomas*

Genotype			c-Met	Pax7	MyoD	Trp53	Cyclin D1	C-MYC	Bcl-XL	Neu	CD44
$Myf6^{ICNm/any}$	$Pax3^{P3Fa/WT}$	—	+++	+	++	++	+++	++	++	0	0
$Myf6^{ICNm/any}$	$Pax3^{P3Fa/P3Fa}$	$Trp53^{F2\text{-}10/WT}$	++	++	++	0	+++	++	++	0	0
$Myf6^{ICNm/any}$	$Pax3^{P3Fa/P3Fa}$	$Trp53^{F2\text{-}10/F2\text{-}10}$	++	+	++	0	+++	++	++	0	0
$Myf6^{ICNm/any}$	$Pax3^{P3Fa/P3Fa}$	$Ink4a/ARF^{F2\text{-}3/F2\text{-}3}$	++	++	++	0	+++	++	++	0	0

Semiquantitative scoring is based on the scale used by Green et al. (1993). In brief, 0 equals no staining, + equals weakly positive staining, ++ equals strongly positive staining equivalent to the control, and +++ equals very strongly positive staining.

mal *Pax3* allele to a *Pax3:Fkhr* allele. In this report, *Pax3:Fkhr* activation was restricted to a target pool of terminally differentiating *Myf6*-expressing skeletal muscle. In $Pax3^{P3Fa/WT}$ $Myf6^{ICNm/WT}$ mice, alveolar rhabdomyosarcomas are rare (1 in 228). However, *Pax3:Fkhr* homozygosity and *Ink4a/ARF* or *Trp53* pathway loss of function significantly accelerates alveolar rhabdomyosarcoma formation from this target pool, raising the interesting possibility that some or most alveolar rhabdomyosarcomas arise from postnatal, terminally differentiating, Myf6-expressing myofibers. However, we cannot rule out the possibility that within the postnatal *Myf6* cell population there is a yet-to-be-identified subpopulation of primitive nondifferentiating myogenic cells, similar to those that transiently express Myf6 in the myotome of the rostral somite but that do not necessarily contribute to embryonic muscle mass (Bober et al. 1991; Summerbell et al. 2002).

These mouse alveolar rhabdomyosarcomas derived from a target pool of maturing myofibers have an immunohistochemical profile that closely parallels human alveolar rhabdomyosarcomas, including a markedly disregulated array of early myogenic marker expression (e.g., myogenin, MyoD, and Pax7), known Pax3:Fkhr targets (e.g., c-Met, Bcl-XL), and markers of proliferation (e.g., C-Myc and Cyclin D1). Because of this immunohistochemical similarity, the inherited immunocompetency of the conditional mouse model, and the ability to form tumors in situ, that is, from a normal muscle environment, this model promises to be valuable for studies of tumor biology as well as for preclinical therapeutic testing.

For the paradigm of accurately modeling translocation-mediated tumor initiation, there are four significant genetic changes to take into account with each fusion. In the case of the t(2;13) translocation in alveolar rhabdomyosarcomas, two fusion genes are created: *Pax3:Fkhr* and *Fkhr:Pax3*. Whereas *Pax3:Fkhr* is consistently transcribed in tumors and is composed of functional elements from both *Pax3* and *Fkhr* (Arndt and Crist 1999), *Fkhr:Pax3* is expressed in a fraction of tumors tested (Frascella et al. 1998) and consists of only a partial *Fkhr* DNA-binding domain and a partial *Pax3* transactivation domain. The two less appreciated genetic changes associated with t(2;13) are the destruction of one allele of *Pax3* and the destruction of one allele of *Fkhr*. Whereas *Pax3* haploinsufficiency is known to cause Waardenburg Syndrome in humans (Tassabehji et al. 1993), a condition not associated with rhabdomyosarcomas or tumorigenesis, the effects of haploinsufficiency of the putative tumor suppressor *Fkhr* are unknown. To test the hypothesis that haploinsufficiency of the tumor suppressor *Fkhr* may, indeed, be associated with the initiation and/or progression of alveolar rhabdomyosarcoma, we introduced a conditional knockout allele of *Fkhr* into $Pax3^{P3Fa/WT}$ $Myf6^{ICNm/WT}$ mice. For this model, *Fkhr* haploinsufficiency does not appear to significantly accelerate tumorigenesis in $Pax3^{P3Fa/WT}$ $Fkhr^{F2\text{-}3m/WT}$ $Myf6^{ICNm/WT}$ animals. However, we have experiments ongoing to determine whether *Fkhr* haploinsufficiency, as a downstream effector of PTEN, acts synergistically with Ink4a/ARF or Trp53 loss of function in the acceleration of rhabdomyosarcomagenesis.

In our model, tumors most often arise from mice homozygous for the *Pax3:Fkhr* allele (although the animal without *Trp53* or *Ink4a/ARF* knockout alleles that developed a tumor at age 12 mo was heterozygous for *Pax3:Fkhr*). This observation raises the possibility that dosage of the *Pax3:Fkhr* knock-in allele is important for tumor initiation, and that in our construction of the knock-in allele, albeit as carefully as was possible, we were missing an important positive *cis*-regulatory element from the *Fkhr* 3′ genomic region, or we did not eliminate an important negative *cis*-regulatory element from the *Pax3* 3′ genomic region. Alternatively, it may simply be a result from species-specific levels of transcription from the *Pax3* locus. This will be an area of further investigation.

It had been an open question whether alveolar rhabdomyosarcomas initiate before or after birth, and whether certain subsets of myogenic progenitors are more susceptible to give rise to this malignancy. Pediatric cancers are frequently associated with translocations, and these translocations are often asymptomatic at birth (Greaves and Wiemels 2003). In the accompanying manuscript (Keller et al. 2004), we have described the embryonic and postnatal consequences of *Pax3:Fkhr* expression within subsets of the *Pax3* expression domain. These results suggest a framework for the molecular gains of function for *Pax3:Fkhr*, as well as the potential cell(s) of origin for alveolar rhabdomyosarcomas. The severity of birth defects in $Pax3^{P3Fa/wt}$ $RajCreTg^{Cre/wt}$ or $Pax3^{P3Fa/wt}$ $Pax7^{ICNm/wt}$ mice and associated lethality suggest that the translocation event in humans is unlikely to occur either as a germ-line mutation or as a mosaic in a broad range of embryonic myogenic precursors. Based on their normal capacity for self-renewal and proliferation during postnatal myogenesis and muscle repair, postnatal multipotent stem cells in muscle (e.g., side population cells) and committed muscle stem cells (i.e., satellite cells) are theoretically the best candidates for being the cells of origin for alveolar rhabdomyosarcomas, but until now the theory has not been tested.

Results from our accompanying paper (Keller et al. 2004) go on to demonstrate that $Pax3^{P3Fa/wt}$ $Pax7^{ICNm/wt}$ mice carrying the activated *Pax3:Fkhr* allele in the Pax7+ prenatal and postnatal satellite cell pools do not develop tumors even up to 3.5 mo of age, well into the young adulthood of these mice. By inference from this experiment for which $Pax3^{P3Fa/wt}$ $Pax7^{ICNm/wt}$ mice have a severely diminished satellite cell pool and inhibited Pax7 target gene activation, formation of the human 2;13 chromosomal translocation should occur in embryonic or neonatal muscle lineages only after normal *Pax*7 expression is no longer critical for establishment or renewal of the satellite cell pool, such as during myoblast differentiation following the postnatal response to muscle injury—or the translocation should occur in only a small minority of Pax7+ satellite cells.

Our results in this report raise the interesting possi-

bility that terminally differentiating skeletal muscle myofibers have the capacity to give rise to alveolar rhabdomyosarcomas, which, in turn, can express markers (myogenin, MyoD, Pax7) of earlier myogenic precursors. This result may not be surprising given that fully differentiated mature skeletal muscle has been demonstrated to have the capacity to dedifferentiate into earlier precursor myogenic forms or even into different lineages (Odelberg et al. 2000). One might expect that for a terminally differentiated cell to begin replicating, loss of cell cycle checkpoint would be necessary, consistent with the fact that a quarter of human rhabdomyosarcomas have aberrant or absent Trp53 (Felix et al. 1992) or Ink4a/ARF (Iolascon et al. 1996) expression. Furthermore, growing evidence from non-alveolar rhabdomyosarcoma mouse models suggests that mutations affecting cell cycle control significantly increase rhabdomyosarcoma frequency for mice with aberrant growth factor expression (see Supplementary Table 1). With regard to cell(s) of origin, the resulting loss of replicative checkpoint(s) would perhaps be advantageous to the expansion of a myogenic precursor transforming into rhabdomyosarcoma, but would be critical to rhabdomyosarcoma arising from terminally differentiating myofibers in quiescence. We therefore postulate that many but perhaps not all human *Pax3:Fkhr*-expressing alveolar rhabdomyosarcomas are derived from differentiating myofibers. These cells would presumably require cell cycle checkpoint loss of function.

In summary, we report a mouse model of alveolar rhabdomyosarcoma, which has been generated by conditional activation of *Pax3:Fkhr* and conditional inactivation of the Trp53 pathway in a target pool of terminally differentiating, *Myf6*-expressing skeletal muscle. This report provides the starting point for understanding the initiation and progression of this tumor and its potential cell(s) of origin. Furthermore, this conditional genetic model will be a valuable tool for understanding the unique biology of alveolar rhabdomyosarcomas and will serve as an exciting new preclinical platform for testing new therapeutic strategies.

Materials and methods

Genomic clones isolation

Genomic DNA clones were isolated from a λ bacteriophage library of mouse strain SvJ-129 (Stratagene). These clones consisted of a 14.2-kb clone spanning intron 7 to the 3′ untranslated region of *Pax3*, an 18.9-kb clone spanning intron 2 to the 3′ untranslated region of *Fkhr*, and a 12-kb clone spanning exon 8 and the 3′ untranslated region of *Myf6*.

Targeted mouse line production

For the *Pax3:Fkhr* conditional mouse line, a targeting vector was constructed for which LoxP sites flank exons 8–10 of *Pax3* at AflII and BstXI sites, respectively. The compact polyadenylation signal and transcriptional pause elements from the *Complement2* gene 3′ untranslated region (Ashfield et al. 1991; Moreira et al. 1995) is inserted upstream of the native *Pax3* polyadenylation signal and the 3′ LoxP site. The 3′ LoxP site is followed by *Fkhr* genomic DNA containing 338 bp of intron 1, 2.9 kb containing exon 2/intron 2/exon 3, and 6.5 kb of the 3′ untranslated region and genomic DNA. An internal ribosome entry site from encephalomyocardial virus and the enhanced yellow fluorescent protein *eYfp* were inserted in exon 3 at a BglII site. This targeting vector was electroporated into R1 embryonic stem cells (Nagy et al. 1993), and the cells were subjected to positive and negative selection (Mansour et al. 1988). Genomic DNA from 144 colonies was analyzed by Southern hybridization using a 3′ external probe to identify 12 clones with a targeted modification of the *Pax3* locus. Southern hybridization using an internal probe and EcoRI-digested genomic DNA was used to further identify three clones that contained the desired 5′ LoxP site from the targeting vector. Cells from these three recombinant clones were microinjected into C57BL/6 blastocysts to generate chimeric mice. Chimeric mice were mated to C57BL/6 females, and their Agouti offspring were tested by Southern hybridization to confirm germ-line transmission of the *Pax3:Fkhr* conditional allele. The FRT-flanked *neomycin resistance* gene (*Neo*) was removed by breeding $Pax3^{P3Fp/wt}$ mice to transgenic mice expressing *Flp-e* (Rodriguez et al. 2000), thereby generating $Pax3^{P3Fm/wt}$ mice.

For the *Fkhr* conditional knockout mouse line, a targeting vector was constructed for which Lox511 sites flank exons 2 and 3 of the *Fkhr* gene. This targeting vector was electroporated into R1 embryonic stem cells subjected to positive and negative selection. Genomic DNA from 71 colonies was analyzed by Southern hybridization using a 3′ external probe to identify 41 clones with a targeted modification of the *Fkhr* locus. Chimeric and germ-line mice were produced as discussed above.

For the *Myf6–Cre* mouse line, a targeting vector was constructed that placed an *ires–Cre–FRT–Neo–FRT* cassette at an engineered XhoI site within the untranslated region of the third exon of the *Myf6* gene, 226 bp after the stop codon. This targeting vector shown in Figure 1C was electroporated into R1 embryonic stem cells subjected to positive and negative selection. Two of 70 clones were identified as positive by screening with AflII, NcoI DNA digests and Southern hybridization using a 5′ external probe, as demonstrated by a downshift from 11.2 to 7.3 kb (data not shown). Chimeric and germ-line mice were produced as discussed above.

Genotyping

Mice carrying targeted alleles were genotyped by PCR. For the *Pax3:Fkhr* mouse line, the 5′ and 3′ primers were ck82, 5′-GGA TTGCATGGTTGGGATGTAGCTG-3′; ck83, 5′-CAAAGAAG CAACAGAGGGAGATG-3′; and ck10 5′-TGAGCATCCAC CAAGAACTC-3′; respectively. DNA was extracted from tails, and 2 µL (5–20 ng) was used in the subsequent PCR reaction. Each 25 µL of PCR reaction contained 1× buffer, 2.5 mM $MgCl_2$, 200 µM deoxynucleotides, 0.6 µM ck82, 0.3 µM ck83, 0.3 µM ck10, and 0.75 U of Taq DNA polymerase (Promega). The cycling conditions were 5 min at 95°C, 27 cycles of 30 sec at 95°C/20 sec at 64°C/60 sec at 72°C, followed by 7 min at 72°C. The wild-type, P3Fm, or P3Fa alleles resulted in 196-bp, 250-bp, or 575-bp bands, respectively.

For genotyping *Fkhr* mouse lines, the 5′ and 3′ primers were ck142, 5′-CCTTCAGAGCTGCCAGGTGAATATG-3′ and ck143, 5′-TGTAGAGAGTATGCCGTCCAGAGTGG-3′; ck30, 5′-GTGTACAAACCAGCTGAGCAC-3′; respectively. Reaction conditions were as described above except that 0.4 µM each primer was used. Cycling conditions were 5 min at 95°C, 32 cycles of 30 sec at 95°C/20 sec at 64°C/60 sec at 72°C, fol-

lowed by 7 min at 72°C. The wild-type, F2-3p, or F2-3m alleles resulted in 290-bp, 350-bp, or 661-bp bands, respectively.

For genotyping *Myf6–Cre* mouse lines, the 5′ and 3′ primers were ck219, 5′-CTTCAGCGCCTTTCTTCCATCG-3′; ba86, 5′-GGATAGTGAAACAGGGCAA-3′; and ba88, 5′-GAACTT CGTTTGCAACTGAC-3′; ba97, 5′-GATCTGGACGAAGAG CATCA-3′; respectively. Reaction conditions were as described above except that 0.8 µM each primer was used. Cycling conditions were the same as for *Pax3:Fkhr*. The wild-type, ICNm, and ICNp alleles resulted in 398-bp, 300-bp, or 550-bp bands, respectively.

Testing Myf6 driver expression

Whole-mount detection of the tissue-specific CRE expression for the *Myf6–Cre* mouse line was performed by crossing that line to *ROSA26* LacZ reporter mice (Sorriano 1999). Embryos were harvested at E15.5 and processed as previously described (Arenkiel et al. 2003).

Detection of Pax3:Fkhr *rearrangements in various tissues*

Genotyping as described above was performed on various tissues from 6-week-old mice with the genotype $Pax3^{P3Fa/WT}$ $Myf6^{ICNm/WT}$ to determine the spectrum of *Myf6–Cre*-driven recombination for the *Pax3:Fkhr* knock-in allele. For each organ, 200 mg of tissue was diced and digested overnight in 330 µg/mL proteinase-K in 100 mM NaCl, 20 mM Tris-Cl (pH 7.6), 10 mM EDTA, and 0.5% SDS. The following day, samples were extracted with phenol, extracted with chloroform, and precipitated with 2.5 volumes of ethanol. Samples were resuspended in TE, and 50 ng was used for the *Pax3:Fkhr* PCR genotyping reaction described above.

Detection of Pax3:Fkhr *transcripts and* eYFP *marker gene*

For epifluorescence microscopy of skeletal muscle for *Pax3:Fkhr* mice, 6-week-old animals were killed by CO_2 asphyxiation and perfused with PBS. The vastus lateralis muscle was dissected and fixed in 4% paraformaldehyde in PBS for 3 h at 4°C. The tissue was washed for 10 min in cold PBS four times, then transitioned from 10% to 20%–30% sucrose in PBS at 60-min intervals. The tissue was embedded in OCT compound (Sakura Finetek U.S.A., Inc.) and snap-frozen on dry ice. Ten-micron-thick cross-sections were subsequently washed in 0.5% Triton X-100 in PBS and coverslipped using FluorMount-G mounting media (Southern Biotech). Slides were visualized with a Zeiss Axiovert 200M epifluorescence microscope using a yfp filter.

Histology and immunohistochemistry of tumors

Histology was performed as previously described (Boulet and Capecchi 2004). Immunohistochemistry for myogenin, smooth muscle actin, muscle-specific actin, Cyclin D1, C-Myc, and Bcl-XL was performed by ARUP Laboratories at the University of Utah on 3.5-µm sections. A rabbit anti-mouse F_{AB2} secondary antibody (Dako Corp.) was used to avoid cross-reactivity with nonspecific mouse tissue antigens. For Pax7, MyoD, and myogenin immunohistochemistry on frozen skeletal muscle (prepared as described in the previous paragraph), staining was performed using the M.O.M. Immunodection Kit Staining Procedure (Vector Laboratories) following the manufacturer's instructions, without antigen unmasking. The Pax7 monoclonal primary antibody (Pax7; Developmental Hybridoma Studies Bank, Iowa City, IA) was used at a concentration of 1:10. The MyoD polyclonal primary antibody (PRB-106C; Covance Corp.) was used at a concentration of 1:3000. The myogenin monoclonal primary antibody (M3559; DAKO Corp.) was used at a concentration of 1:50. Slides were coverslipped with Fluoromount-G (Southern Biotechnology Associates) or DAPI mounting medium (Vector Laboratories) and visualized by standard light microscopy. Immunohistochemistry using rabbit polyclonal anti-Pax3 (Li et al. 1999) (a kind gift from J. Epstein, University of Pennsylvania, Philadelphia, PA), and rabbit polyclonal anti-cMet (Jeffers et al. 1997) (a kind gift from G. Vande-Woude, Van Andel Research Institute, Grand Rapids, MI) were performed as previously described.

Computed tomography scanning

Computed tomography of sacrificed mice was performed at 93 μm^3 voxel resolution using an eXplore Locus Small Animal MicroCT Scanner (GE Healthcare). Images were reconstructed and visualized with the manufacturer's MicroView freeware.

Acknowledgments

The Pax7 antibody developed by Atsushi Kawakami was obtained from the Developmental Studies Hybridoma Bank (University of Iowa). We thank Anton Berns for Trp53 conditional knockout mice. We thank Mark Hansen, Lance Burrell, Sheryl Tripp, Michael Thorton, and P.J. Hawkes for technical assistance. This work was supported by a K08 award to C.K. from the National Cancer Institute (1K08 CA90438-01) and a Cancer Center Support Pilot Grant (NCI P30 CA42014). We thank the Huntsman Cancer Institute Center for Children and the University of Utah Sarcoma Service for ongoing support.

References

Aguirre, A.J., Bardeesy, N., Sinha, M., Lopez, L., Tuveson, D.A., Horner, J., Redston, M.S., and DePinho, R.A. 2003. Activated Kras and Ink4a/Arf deficiency cooperate to produce metastatic pancreatic ductal adenocarcinoma. *Genes & Dev.* **17:** 3112–3126.

Anderson, M.J., Shelton, G.D., Cavenee, W.K., and Arden, K.C. 2001. Embryonic expression of the tumor-associated PAX3–FKHR fusion protein interferes with the developmental functions of Pax3. *Proc. Natl. Acad. Sci.* **98:** 1589–1594.

Arenkiel, B.R., Gaufo, G.O., and Capecchi, M.R. 2003. Hoxb1 neural crest preferentially form glia of the PNS. *Dev. Dyn.* **227:** 379–386.

Arndt, C.A. and Crist, W.M. 1999. Common musculoskeletal tumors of childhood and adolescence. *New Eng. J. Med.* **341:** 342–352.

Ashfield, R., Enriquez-Harris, P., and Proudfoot, N.J. 1991. Transcriptional termination between the closely linked human complement genes C2 and Factor B: Common termination factor for C2 and c-myc? *EMBO J.* **10:** 4197–4207.

Barr, F.G., Galili, N., Holick, J., Biegel, J.A., Rovera, G., and Emanuel, B.S. 1993. Rearrangement of the PAX3 paired box gene in the paediatric solid tumor alveolar rhabdomyosarcoma. *Nat. Genet.* **3:** 113–117.

Bober, E., Lyons, G.E., Braun, T., Cossu, G., Buckingham, M., and Arnold, H.-H. 1991. The muscle regulatory gene, Myf-6, has a biphasic pattern of expression during early mouse development. *J. Cell Biol.* **113:** 1255–1265.

Boulet, A.M. and Capecchi, M.R. 2004. Multiple roles of Hoxa11 and Hoxd11 in the formation of the mammalian forelimb zeugopod. *Development* **131:** 299–309.

Braun, T. and Arnold, H.-H. 1995. Inactivation of Myf-6 and Myf-5 genes in mice leads to alterations in skeletal muscle

development. *EMBO J.* **14:** 1176–1186.
Cavenee, W.K. 2002. Muscling in on rhabdomyosarcoma. *Nat. Med.* **8:** 1200–1201.
Cornelison, D.D. and Wold, B.J. 1997. Single-cell analysis of regulatory gene expression in quiescent and activated mouse skeletal muscle satellite cells. *Dev. Biol.* **191:** 270–283.
Felix, C.A., Kappel, C.C., Mitsudomi, T., Nau, M.M., Tsokos, M., Crouch, G.D., Nisen, P.D., Winick, N.J., and Helman, L.J. 1992. Frequency and diversity of p53 mutations in childhood rhabdomyosarcoma. *Cancer Res.* **52:** 2243–2247.
Fleischmann, A., Jochum, W., Eferl, R., Witowsky, J., and Wagner, E.F. 2003. Rhabdomyosarcoma development in mice lacking Trp53 and Fos: Tumor suppression by the Fos protooncogene. *Cancer Cell* **4:** 477–482.
Forster, A., Pannell, R., Drynan, L.F., McCormack, M., Collins, E.C., Daser, A., and Rabbitts, T.H. 2003. Engineering de novo reciprocal chromosomal translocations associated with Mll to replicate primary events of human cancer. *Cancer Cell* **3:** 449–458.
Frascella, E., Toffolatti, L., and Rosolen, A. 1998. Normal and rearranged PAX3 expression in human rhabdomyosarcoma. *Cancer Genet. Cytogenet.* **102:** 104–109.
Ginsberg, J.P., Davis, R.J., Bennicelli, J.L., Nauta, L.E., and Barr, F.G. 1998. Up-regulation of MET but not neural cell adhesion molecule expression by the PAX3–FKHR fusion protein in alveolar rhabdomyosarcoma. *Cancer Res.* **58:** 3542–3546.
Goulding, M., Sterrer, S., Fleming, J., Balling, R., Nadeau, J., Moore, K.J., Brown, S.D., Steel, K.P., and Gruss, P. 1993. Analysis of the Pax-3 gene in the mouse mutant splotch. *Genomics* **17:** 355–363.
Greaves, M.F. and Wiemels, J. 2003. Origins of chromosome translocations in childhood leukaemia. *Nat. Rev. Cancer* **3:** 639–649.
Green, J.A., Robertson, L.J., and Clark, A.H. 1993. Glutathione S-transferase expression in benign and malignant ovarian tumors. *Br. J. Cancer* **68:** 235–239.
Grundy, R., Anderson, J., Gaze, M., Gerrard, M., Glaser, A., Gordon, A., Malone, M., Pritchard-Jones, K., and Michalski, A. 2001. Congenital alveolar rhabdomyosarcomam. *Cancer* **91:** 606–612.
Gurney, J.G., Young Jr., J.L., Roffers, S.D., Smith, M.A., and Bunin, G.R. 1999. Soft tissue sarcomas. In *Cancer incidence and survival among children and adolescents: United States SEER Program 1975–1995, National Cancer Institute, SEER Program, NIH Pub. No. 99-4649* (eds. S.M. Ries LAG et al.), pp. 111–124. National Cancer Institute, Bethesda, MD.
Hosaka, T., Biggs III, W.H., Tieu, D., Boyer, A.D., Varki, N.M., Cavenee, W.K., and Arden, K.C. 2004. Disruption of forkhead transcription factor (FOXO) family members in mice reveals their functional diversification. *Proc. Natl. Acad. Sci.* **101:** 2975–2980.
Hsu, Y.T., Wolter, K.G., and Youle, R.J. 1997. Cytosol-to-membrane redistribution of Bax and Bcl-X(L) during apoptosis. *Proc. Natl. Acad. Sci.* **94:** 3668–3672.
Humphrey, G., Hazel, D.L., MacLennan, K., and Lewis, I. 1999. Expression of CD44 by rhabdomyosarcoma: A new prognostic marker? *Br. J. Cancer* **80:** 918–921.
Iolascon, A., Faienza, M.F., Coppola, B., Rosolen, A., Basso, G., Della Ragione, F., and Schettini, F. 1996. Analysis of cyclin-dependent kinase inhibitor genes (CDKN2A, CDKN2B, and CDKN2C) in childhood rhabdomyosarcoma. *Genes Chrom. Cancer* **15:** 217–222.
Jacks, T., Remington, L., Williams, B.O., Schmitt, E.M., Halachmi, S., Bronson, R.T., and Weinberg, R.A. 1994. Tumor spectrum analysis in p53-mutant mice. *Curr. Biol.* **4:** 1–7.
Jeffers, M., Schmidt, L., Nakaigawa, N., Webb, C.P., Weirich, G., Kishida, T., Zbar, B., and Vande Woude, G.F. 1997. Activating mutations for the met tyrosine kinase receptor in human cancer. *Proc. Natl. Acad. Sci.* **94:** 11445–11450.
Jonkers, J., Meuwissen, R., van der Gulden, H., Peterse, H., van der Valk, M., and Berns, A. 2001. Synergistic tumor suppressor activity of BRCA2 and p53 in a conditional mouse model for breast cancer. *Nat. Genet.* **29:** 418–425.
Keller, C., Hansen, M.S., Coffin, C.M., and Capecchi, M.R. 2004. *Pax3:Fkhr* interferes with embryonic *Pax3* and *Pax7* function: Implications for alveolar rhabdomyosarcoma cell of origin. *Genes & Dev.* (this issue).
Kirkwood, T.B. 2002. p53 and ageing: Too much of a good thing? *Bioessays* **24:** 577–579.
Kouraklis, G., Triche, T.J., Wesley, R., and Tsokos, M. 1999. Myc oncogene expression and nude mouse tumorigenicity and metastasis formation are higher in alveolar than embryonal rhabdomyosarcoma cell lines. *Pediatric Res.* **45:** 552–558.
Lagutina, I., Conway, S.J., Sublett, J., and Grosveld, G.C. 2002. Pax3–FKHR knock-in mice show developmental aberrations but do not develop tumors. *Mol. Cell Biol.* **22:** 7204–7216.
Li, F.P. and Fraumeni Jr., J.F. 1969. Rhabdomyosarcoma in children: Epidemiologic study and identification of a familial cancer syndrome. *J. Natl. Cancer Inst.* **43:** 1365–1373.
Li, J., Liu, K.C., Jin, F., Lu, M.M., and Epstein, J.A. 1999. Transgenic rescue of congenital heart disease and spina bifida in Splotch mice. *Development* **126:** 2495–2503.
Mansour, S.L., Thomas, K.R., and Capecchi, M.R. 1988. Disruption of the proto-oncogene int-2 in mouse embryo-derived stem cells: A general strategy for targeting mutations to nonselectable genes. *Nature* **336:** 348–352.
Margue, C.M., Bernasconi, M., Barr, F.G., and Schafer, B.W. 2000. Transcriptional modulation of the anti-apoptotic protein BCL-XL by the paired box transcription factors PAX3 and PAX3/FKHR. *Oncogene* **19:** 2921–2929.
Mark, H.F., Brown, S., Sun, C.L., Samy, M., and Afify, A. 1998. Fluorescent in situ hybridization detection of HER-2/neu gene amplification in rhabdomyosarcoma. *Pathobiology* **66:** 59–63.
Moreira, A., Wollerton, M., Monks, J., and Proudfoot, N.J. 1995. Upstream sequence elements enhance poly(A) site efficiency of the C2 complement gene and are phylogenetically conserved. *EMBO J.* **14:** 3809–3819.
Nagy, A., Rossant, J., Nagy, R., Abramow-Newerly, W., and Roder, J.C. 1993. Derivation of completely cell culture-derived mice from early-passage embryonic stem cells. *Proc. Natl. Acad. Sci.* **90:** 8424–8428.
Nanni, P., Nicoletti, G., De Giovanni, C., Croci, S., Astolfi, A., Landuzzi, L., Di Carlo, E., Iezzi, M., Musiani, P., and Lollini, P.L. 2003. Development of rhabdomyosarcoma in HER-2/neu transgenic p53 mutant mice. *Cancer Res.* **63:** 2728–2732.
Nilsson, J.A. and Cleveland, J.L. 2003. Myc pathways provoking cell suicide and cancer. *Oncogene* **22:** 9007–9021.
Odelberg, S.J., Kollhoff, A., and Keatin, M.T. 2000. Dedifferentiation of mammalian myotubes induced by msx1. *Cell* **103:** 1099–1109.
Olson, E.N., Arnold, H.H., Rigby, P.W., and Wold, B.J. 1996. Know your neighbors: Three phenotypes in null mutants of the myogenic bHLH gene MRF4. *Cell* **85:** 1–4.
Qualman, S.J., Coffin, C.M., Newton, W.A., Hojo, H., Triche, T.J., Parham, D.M., and Crist, W.M. 1998. Intergroup rhabdomyosarcoma study: Update for pathologists. *Pediatr. Dev. Pathol.* **1:** 550–561.
Relaix, F., Polimeni, M., Rocancourt, D., Ponzetto, C., Schafer, B.W., and Buckingham, M. 2003. The transcriptional activa-

tor PAX3-FKHR rescues the defects of Pax3 mutant mice but induces a myogenic gain-of-function phenotype with ligand-independent activation of Met signaling in vivo. *Genes & Dev.* **17:** 2950–2965.

Rodriguez, C.I., Buchholz, F., Galloway, J., Sequerra, R., Kasper, J., Ayala, R., Stewart, A.F., and Dymecki, S.M. 2000. High-efficiency deleter mice show that FLPe is an alternative to Cre-loxP [letter]. *Nat. Genet.* **25:** 139–140.

Sharp, R., Recio, J.A., Jhappan, C., Otsuka, T., Liu, S., Yu, Y., Liu, W., Anver, M., Navid, F., Helman, L.J., et al. 2002. Synergism between INK4a/ARF inactivation and aberrant HGF/SF signaling in rhabdomyosarcomagenesis. *Nat. Med.* **8:** 1276–1280.

Sorensen, P.H., Lynch, J.C., Qualman, S.J., Tirabosco, R., Lim, J.F., Maurer, H.M., Bridge, J.A., Crist, W.M., Triche, T.J., and Barr, F.G. 2002. PAX3–FKHR and PAX7–FKHR gene fusions are prognostic indicators in alveolar rhabdomyosarcoma: A report from the children's oncology group. *J. Clin. Oncol.* **20:** 2672–2679.

Sorriano, P. 1999. Generalized lacZ expression with the ROSA26 Cre reporter strain. *Nat. Genet.* **21:** 70–71.

Summerbell, D., Halai, C., and Rigby, P.W. 2002. Expression of the myogenic regulatory factor Mrf4 precedes or is contemporaneous with that of Myf5 in the somitic bud. *Mech. Dev.* **117:** 331–335.

Takahashi, Y., Oda, Y., Kawaguchi, K., Tamiya, S., Yamamoto, H., Suita, S., and Tsuneyoshi, M. 2004. Altered expression and molecular abnormalities of cell-cycle-regulatory proteins in rhabdomyosarcoma. *Mod. Pathol.* **17:** 660–669.

Tassabehji, M., Read, A.P., Newton, V.E., Patton, M., Gruss, P., Harris, R., and Strachan, T. 1993. Mutations in the PAX3 gene causing Waardenburg syndrome type 1 and type 2. *Nat. Genet.* **3:** 26–30.

Tiffin, N., Williams, R.D., Shipley, J., and Pritchard-Jones, K. 2003. PAX7 expression in embryonal rhabdomyosarcoma suggests an origin in muscle satellite cells. *Br. J. Cancer* **89:** 327–332.

Tomescu, O., Xia, S.J., Strezlecki, D., Bennicelli, J.L., Ginsberg, J., Pawel, B., and Barr, F.G. 2004. Inducible short-term and stable long-term cell culture systems reveal that the PAX3–FKHR fusion oncoprotein regulates CXCR4, PAX3, and PAX7 expression. *Lab. Invest.* **84:** 1060–1070.

Tonin, P.N., Scrable, H., Shimada, H., and Cavenee, W.K. 1991. Muscle-specific gene expression in rhabdomyosarcomas and stages of human fetal skeletal muscle development. *Cancer Res.* **51:** 5100–5106.

Wexler, L.H. and Helman, L.J. 1997. Rhabdomyosarcoma and the undifferentiated sarcomas. In *Principles and practice of pediatric oncology* (eds. P.A. Pizzo and D.G. Poplack), pp. 799–829. Lippincott-Raven, Philadelphia.